

UNCLASSIFIED

AD 4 4 6 1 6 9

DEFENSE DOCUMENTATION CENTER

FOR

SCIENTIFIC AND TECHNICAL INFORMATION

CAMERON STATION, ALEXANDRIA, VIRGINIA



UNCLASSIFIED

NOTICE: When government or other drawings, specifications or other data are used for any purpose other than in connection with a definitely related government procurement operation, the U. S. Government thereby incurs no responsibility, nor any obligation whatsoever; and the fact that the Government may have formulated, furnished, or in any way supplied the said drawings, specifications, or other data is not to be regarded by implication or otherwise as in any manner licensing the holder or any other person or corporation, or conveying any rights or permission to manufacture, use or sell any patented invention that may in any way be related thereto.

ADVISORY GROUP FOR AERONAUTICAL RESEARCH AND DEVELOPMENT

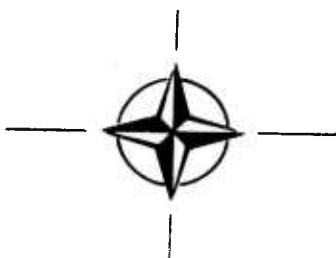
64 RUE DE VARENNE, PARIS VII

APRIL 1961

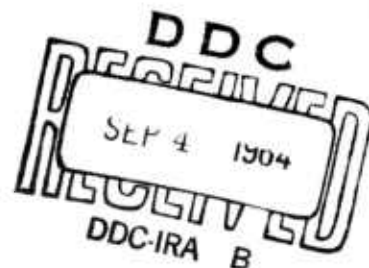
**STATIC AND DYNAMIC STABILITY
OF BLUNT BODIES**

by

H. C. DUBOSE

REPORT 347

NORTH ATLANTIC TREATY ORGANISATION



62-08-5384

NORTH ATLANTIC TREATY ORGANIZATION

5 ADVISORY GROUP FOR AERONAUTICAL RESEARCH AND DEVELOPMENT

Paris

(France).

6 STATIC AND DYNAMIC STABILITY
OF BLUNT BODIES,

10 by

H.C. DuBose,

This Report is one in the Series 334-374, inclusive, presenting papers, with discussions, given at the AGARD Specialists' Meeting on 'Stability and Control', Training Center for Experimental Aerodynamics, Rhode-Saint-Genèse, Belgium, 10-14 April 1961, sponsored jointly by the AGARD Fluid Dynamics and Flight Mechanics Panels



SUMMARY

~~This is~~ A description is given of the relationships between the flow fields and the static and dynamic stability of blunted-cone-cylinder-flare type re-entry bodies at Mach numbers from 0.7 to 5.0. Effects of variations in some of the shape parameters on the dynamic stability are presented. It is shown that certain combinations of cone and flare angles result in instability in the transonic range. Also, comparison is made between free and forced oscillation data.



SOMMAIRE

Une description est donnée des rapports entre les champs d'écoulement et la stabilité statique et dynamique des corps de rentrée du type à cône émoussé-cylindre-renflement aux nombres de Mach compris entre 0,7 et 5. L'influence sur la stabilité dynamique de variations de certains des paramètres de forme est exposée. Il est démontré que certaines combinaisons des angles de cône et de renflement provoquent l'instabilité dans la gamme des vitesses transsoniques. En plus, les résultats d'essais effectués avec des oscillations libres sont comparés à ceux obtenus avec des oscillations forcées.

533.6.013.4:533.696

3c6e7:3b3g2

CONTENTS

	Page
SUMMARY	ii
LIST OF FIGURES	iv
NOTATION	v
1. INTRODUCTION	1
2. APPARATUS	1
2.1 Wind Tunnels	1
2.2 Balances	1
3. TESTS AND RESULTS	2
3.1 Flow Characteristics	2
3.2 Static Stability	2
3.3 Dynamic Stability	4
4. CONCLUSIONS	6
REFERENCES	7
FIGURES	8
DISCUSSION	A-i
ADDENDUM: Complete List of Papers in Series	
DISTRIBUTION	

LIST OF FIGURES

		Page
Fig. 1	Dynamic support, propulsion wind tunnel	8
Fig. 2	Forced-oscillation balance, propulsion wind tunnel	9
Fig. 3	Typical blunted-cone-cylinder-flare configuration with pressure distribution	10
Fig. 4	Schlieren photographs of flow field	11
Fig. 5	Effect of Mach number on variation of pitching moment coefficient with angle of attack	12
Fig. 6	Effect of Reynolds number and surface roughness on neutral point location	13
Fig. 7	Typical variation of $C_{m\alpha}$ with Mach number	14
Fig. 8	Typical variation of $C_{m\dot{\theta}} + C_{m\dot{\alpha}}$ with Mach number	14
Fig. 9	Effect of oscillation amplitude on $C_{m\dot{\theta}} + C_{m\dot{\alpha}}$	15
Fig.10	Effect of Reynolds number on variation of $C_{m\dot{\theta}} + C_{m\dot{\alpha}}$ with Mach number	16
Fig.11	Transonic dynamic stability boundary for typical blunted-cone-cylinder-flare configurations	17
Fig.12	Effect of Reynolds number on flow pattern at $M_\infty = 2.5$	18
Fig.13	Effect of centerbody length on variation of $C_{m\dot{\theta}} + C_{m\dot{\alpha}}$ with Mach number	18
Fig.14	Effect of flare length on variation of $C_{m\dot{\theta}} + C_{m\dot{\alpha}}$ with Mach number	19
Fig.15	Variation of $C_{m\dot{\theta}} + C_{m\dot{\alpha}}$ with body length according to Newtonian impact theory	20
Fig.16	Comparison of $C_{m\dot{\theta}} + C_{m\dot{\alpha}}$ values from free-oscillation and forced-oscillation tests	21
Fig.17	Comparison of limit cycle amplitudes from free-oscillation tests with amplitudes for zero damping from forced-oscillation tests	21

NOTATION

M	pitching moment about designated moment reference, ft-lbs
C_m	pitching-moment coefficient ($= 4M/q_\infty \pi D^3$)
C_{m_α}	static stability parameter ($= \partial C_m / \partial \alpha$ per rad)
$C_{m\dot{\theta}} + C_{m\dot{\alpha}}$	dynamic stability parameter: $\frac{\partial C_m}{\partial (\dot{\theta} D / 2V_\infty)} + \frac{\partial C_m}{\partial (\dot{\alpha} D / 2V_\infty)} \text{ per rad}$
D	model centerbody diameter, ft
M_∞	free-stream Mach number
p_∞	free-stream static pressure, lb/in. ²
q_∞	free-stream dynamic pressure ($= 0.7 p_\infty M_\infty^2$ lb/in. ²)
R	Reynolds number based on model length ($= V_\infty l / \nu_\infty$)
l	model length, ft
V_∞	free-stream velocity, ft/sec
α	angle of attack, deg
$\bar{\alpha}$	amplitude of forced oscillations, deg
α_{lim}	limit-cycle amplitude, deg
$\dot{\alpha}$	rate of change of angle of attack ($= d\alpha/dt$ rad/sec)
θ	angle of pitch relative to tunnel centerline, rad
$\dot{\theta}$	rate of change of pitch angle ($= d\theta/dt$ rad/sec)
ν_∞	free-stream kinematic viscosity, ft ² /sec
x_{np}	neutral point location, positive aft of model nose, ft
t	time, seconds
ω	circular frequency of oscillation, rad/sec
L_c	centerbody length in centerbody diameters

L_t	flare length in centerbody diameters
θ_n	forebody half-angle, deg
θ_t	flare angle, deg

STATIC AND DYNAMIC STABILITY OF BLUNT BODIES

H.C. DuBose*

1. INTRODUCTION

Solutions of the heating and stability problems of atmospheric re-entry together with the problems of packaging useful loads for re-entry flight, have produced a variety of unique blunt-body shapes, all of which were of little or no interest to aerodynamicists a decade ago. Although many of these shapes are geometrically very simple, analytical methods for predicting their aerodynamic characteristics have been somewhat inadequate and, as a result, extensive testing has been given them in wind tunnels and in free flight.

One family of re-entry bodies which has received considerable attention recently is the blunted-cone-cylinder-flare type. These shapes are particularly well suited for certain applications due to their desirable characteristics at hypersonic speeds. However, as will be seen, their low supersonic and transonic characteristics require careful evaluation. It is the purpose of this paper to point out certain general observations concerning the static and dynamic stability of this family of shapes.

2. APPARATUS

2.1 Wind Tunnels

The results presented were obtained from tests in the 1-ft transonic tunnel, the 1-ft supersonic tunnel and the 16-ft transonic circuit of the Propulsion Wind Tunnel Facility, and in tunnel E-1 and tunnel A of the von Kármán Gas Dynamics Facility.

2.2 Balances

Conventional internal strain-gage balances were used for the static tests; for the dynamic tests, both free and forced pitching oscillation type balances were used.

The free-oscillation balances are of the strain-gaged flexure type. Although they range in size from 0.6 inch diameter to 11 inches diameter, the basic design is as shown in Figure 1. The pivot is formed by a vertical flexure in the center and two longitudinal flexures at the sides. A mechanism is provided at the rear of the balance for giving the model an initial angular deflection. The damping is determined from the rate of decay of the amplitude of the pitching oscillations and the static stability may be determined from a comparison of the wind-on and wind-off frequencies.

The forced oscillation balance (Fig. 2) is used in the 16-ft transonic circuit to provide more complete data in cases where the aerodynamic damping is negative or nonlinear. The design was based on an earlier one by the Ames Laboratory of the N.A.S.A.

*Supervisor, Dynamic Projects Section, Arnold Center Propulsion Wind Tunnel Facility, Arnold Air Force Station, Tennessee, U.S.A.

The model is attached to the disc-shaped face of the forward unit which is a strain-gaged balance designed to measure the moment about the pitching axis. The pivot is of the ball-bearing type and the oscillations are controlled by means of an hydraulic actuator. A leaf spring extending through the front face of the balance is strain gaged for angular position read-out. An analog system is provided to resolve the measured moment into two components: one in phase with position and one in quadrature to the position.

3. TESTS AND RESULTS

3.1 Flow Characteristics

A blunted-cone-cylinder-flare shape having relative dimensions typical of those to be discussed is shown in Figure 3. Some general comments can be made about the flow over such a body. The pressure distribution for zero angle of attack over a considerable range of Mach numbers, subsonic, transonic and supersonic, is similar to that shown at the bottom of the figure. From a stagnation point at the nose, the flow expands initially over the cone and then sharply at the corner where the cone and cylinder intersect. This is followed by a relatively gradual compression along the cylinder with additional compression occurring due to the concave junction of the cylinder and flare. It is over the length of the cylinder in the region of adverse pressure gradients that under certain conditions flow separation can occur, introducing problems of considerable importance.

A set of schlieren photographs is presented in Figure 4 to show the nature of the separation. Note that at high subsonic Mach number the flow is separated over the entire cylinder and flare at zero angle of attack. At Mach number one, the flow has become attached around the corner at the cone-cylinder junction and over a small distance along the cylinder. As Mach number is further increased, the separation point moves farther aft along the cylinder and the flow is attached on the flare. For a given Mach number, the effect of angle of attack is to shift the separation point forward on the lee side of the body and aft on the windward side as shown in Figure 4 for $\alpha = -2^\circ$ and $M_\infty = 1$.

3.2 Static Stability

Some results, selected to show the range of consequences of these flow phenomena, are presented in Figure 5, where the static pitching moment coefficient, C_m , is given as a function of angle of attack. For $M_\infty = 0.85$, with completely separated flow at zero angle of attack, the slope is high where the region of separation decreases in extent on the windward side as α increases. For $M_\infty = 1$ where the zero angle of attack flow is attached over a small distance along the cylinder, the C_m vs α slope is initially less. However, as the angle of attack is increased, a point is reached at which the separation point on the lee side moves abruptly forward to the corner at the cone cylinder junction. This is accompanied by a sharp rise in the magnitude of C_m . When angle of attack is decreased from this point, a considerable angle may be traversed with the lee surface remaining completely separated aft of the corner. Reattachment is then accompanied by a relatively sharp drop in the magnitude of C_m . Thus a hysteresis loop is formed. The angle-of-attack extent of the hysteresis loop may be negligible or large depending upon the model configuration and free-stream

conditions. If the loop extends to zero angle of attack, the original condition of attached flow on the forward part of the cylinder at zero angle of attack may not recur. In this case, the original conditions can be re-established if Mach number is first increased until re-attachment occurs, and then decreased to the desired value. Thus, in the wind tunnel test a 'Mach number hysteresis' may also be encountered.

The relatively large magnitudes of the pitching moment coefficient at small angles of attack, and consequent steep slopes, $C_{m\alpha}$, are typical at high subsonic and low supersonic stream velocities. As indicated previously, this results when the state of the flow progresses from a zero-angle-of-attack condition of either complete separation in the subsonic case, or attachment in the supersonic case, to an angle-of-attack condition of attached flow on the windward side and separated flow on the lee side. Experimental pressure distributions show that the loads producing the large stable pitching moment act primarily on the flare, and result from lower pressures in the separated flow on the lee side.

At higher Mach numbers where the region of separation is absent or very small at zero angle of attack, the slope of C_m vs α is small in magnitude and usually constant throughout a considerable range of angle of attack as shown in the case for $M_\infty = 1.5$ in Figure 5.

The static stability of blunted-cone-cylinder-flare bodies has been investigated extensively in the Mach number range 0.7 to 5.0 by Rittenhouse and Kaupp, of the Arnold Center, who have shown a number of interesting characteristics. As might be expected, for Mach numbers throughout the range, the neutral point was found to move aft with increasing cylinder length, flare length, and flare angle. With regard to Mach number effects, the neutral point was found to reach its most forward position in the vicinity of Mach number 1.5 for a wide range of shapes. Thus it is this Mach number that normally determines the aft limit of the center of gravity for static stability for $0.7 < M_\infty < 5.0$. Fortuitously, Reynolds number effects were found to be small at Mach numbers from 1.4 to 2.0, where little or no separation was encountered.

At Mach numbers in the transonic range, they found Reynolds number effects to be significant, especially near $M_\infty = 1$, where considerable variation occurs in the extent of the separated region with varying angle of attack. This is illustrated in Figure 6 with a plot of neutral point x_{np} vs Reynolds number. Note that as Reynolds number increases from about two million, the neutral point moves aft rapidly until a Reynolds number of approximately eight million is reached. Pressure distributions indicate that this is associated with a general forward progression of the area of separation; at $R = 8 \times 10^6$ the zero-angle-of-attack flow was separated completely aft of the cone-cylinder junction. A further increase in Reynolds number produced a small forward movement of the neutral point. When a band of surface roughness elements was applied mid-way on the nose, the neutral point shifted to a location near the rear of the body at the lower Reynolds numbers. At a Reynolds number of eight million however, the neutral point was slightly forward of its position for the clean body. Although in this case the effects of either adding roughness elements or increasing Reynolds number were similar, a different result was obtained at $M_\infty = 0.9$. At this Mach number the flow was completely separated at zero angle of attack, and the neutral point was at 83% of the body length for the clean body at $R = 8 \times 10^6$. Increasing the Reynolds number to eighteen million caused the neutral point to move forward to the 76% station. However, with the addition of roughness elements at a Reynolds number

of eight million, the neutral point moved aft to the 90% station. Rittenhouse and Kaupp point out that the boundary layer is thinned by increasing Reynolds number while addition of roughness elements would be expected to thicken the boundary layer, hence different effects might be expected under conditions such as these.

Gray has reported a study of flow separation effects on blunted-cone-cylinder-flare models at Mach numbers of two to five in tunnels E-1 and A (Ref. 1). He shows that the extent of boundary layer separation increases with increasing Mach number in this range, and decreases with increasing Reynolds number. At $M_\infty = 5$ the separated region at zero angle of attack was found to extend over a length greater than the radius of the centerbody at Reynolds numbers as high as eight million. Thus, Reynolds number effects are significant in tests at the higher Mach numbers in the range $2 < M_\infty < 5$ as well as at transonic Mach numbers. However, Gray indicates much better correlation than was obtained in the transonic range between results for high Reynolds numbers and results for low Reynolds numbers with surface roughness elements added.

3.3 Dynamic Stability

To introduce a discussion of some of the dynamic stability results, a plot of pitching-moment-coefficient slope, C_{m_α} , at zero angle of attack for a typical blunted-cone-cylinder-flare configuration is presented in Figure 7. For the moment reference point chosen, the configuration is statically stable except for a small supersonic Mach number range, and exhibits a marked maximum stability in the vicinity of $M_\infty = 1$. Presented in Figure 8 for comparison are dynamic stability results for the same configuration. The ordinate is the pitch damping coefficient $(C_{m\dot{\theta}} + C_{m\dot{\alpha}})$, with negative or stable values above the axis. The data are for a small amplitude of oscillation about zero angle of attack and were obtained with the forced-oscillation balance in the 16-ft transonic circuit. Note that at the Mach number for which the static stability is a maximum, the damping coefficient is positive or unstable and, in general, the damping-coefficient curve is somewhat like a mirror image of the C_{m_α} curve. This is not surprising, since, as pointed out previously, the large magnitudes of C_{m_α} are associated with a flow which exhibits variations in regions of separation and attachment with varying angle of attack. With such characteristics, it is reasonable to assume that there is a lag or hysteresis in the establishment of flow separation and attachment under oscillatory conditions similar to that which has been shown in the case of stall flutter of wings². These results are typical for blunted-cone-cylinder-flare configurations having extensive separation in the vicinity of $M_\infty = 1$. Thus, dynamic instability is a problem with many of these shapes at transonic Mach numbers.

As is the case with the static pitching moment, the damping moment may vary non-linearly with angle of attack in the transonic range. A typical example obtained with the forced-oscillation balance is shown in Figure 9, where the damping coefficient is plotted as a function of the amplitude of oscillation. The data show the damping coefficient to be destabilizing at small amplitudes and stabilizing at large amplitudes. The intermediate amplitude where the damping is zero corresponds to a 'limit cycle' amplitude in free oscillations about the same pitch axis. That is, if the model is released at an angle of attack greater than or less than the limit-cycle amplitude, the oscillations will decay or build up, respectively, to the limit-cycle amplitude. Other forms of non-linear damping have been obtained. For instance, if the C_m vs α hysteresis mentioned previously exists, the configuration may exhibit dynamic stability at small amplitudes and dynamic instability at large amplitudes.

Reynolds number effects on the dynamic stability have been found to be quite strong in the transonic range. Figure 10 presents a plot of damping coefficient vs Mach number for small amplitude oscillations for a typical model. Note that the variation in Reynolds number changed not only the magnitude but also the sign of the damping coefficient at some Mach numbers. Comparison of several shapes at Reynolds numbers from approximately two to twenty million has given results similar to that shown. In general, if a configuration exhibited instability at one Reynolds number in the transonic range, it also exhibited instability at all other Reynolds numbers, although the degree of instability and the Mach number range of instability both varied.

J.A. Black of the Arnold Center has recently completed an investigation of the dynamic stability of blunted-cone-cylinder-flare models of a wide range of shapes at Mach numbers from 0.7 to 3.5. Some of his results showing the relationships between the shape parameters and the dynamic stability are summarized here.

The existence of the transonic dynamic instability was found to depend upon cone angle and flare angle as shown in Figure 11. Flare angle was varied from zero, which is simply an extension of the cylinder, to 15° . For $\theta_n = 10$, no instability was obtained in the transonic range. For $15 \leq \theta_n \leq 20$ the instability could be eliminated by reducing the flare angle, however, for $\theta_n > 25$, the instability was obtained for all flare angles, including zero.

At Mach numbers above and below the range of the transonic instability increasing the flare angle generally produced an increase in the damping. An exception to this was observed at $M_\infty = 2.5$, at low Reynolds numbers only, where instability of the limit cycle type was encountered. Here as in the transonic case, the effect of increasing flare angle was adverse in the respect that a corresponding increase in the limit cycle amplitude was obtained. Schlieren photographs (Fig. 12) showed the instability to be associated with extensive flow separation which disappeared as the Reynolds number was increased. Although the Reynolds numbers at which the instability was obtained were small (0.5×10^6) at this Mach number, the results of Reference 1 with regard to separation seem to indicate that instability might occur at significantly larger Reynolds numbers at $M_\infty > 4$.

Typical effects of centerbody length on the dynamic stability are shown in Figure 13. For the configuration indicated, increasing the cylinder length produced a general increase in the damping and eliminated the instability. Similar effects are shown in Figure 14 for increasing flare length; however, in this case the instability was reduced but not eliminated. To summarize, the effects of increasing the body length are generally favorable for a given forebody.

It has been pointed out by Bauer of the Arnold Center that the increase in damping associated with increasing flare angle, centerbody length, and flare length might have been anticipated from Newtonian theory. Newtonian theory predictions for some configurations having a cone half-angle of 15° are shown in Figure 15. The plot shows how the damping coefficient varies as the length of the configuration is increased by addition of various lengths of cylinder and flare to the blunted-cone forebody. The curve starts at a length equal to that of the forebody with the damping coefficient of the forebody. Since the theory accounts for effects of only those parts of the surface that appear in a frontal projection of the configuration, the surface of the cylinder contributes nothing to the damping, and the curve has zero slope over the

length of the cylinder. At a length corresponding to the beginning of the flare, the damping increases. Since the initial rate of increase varies with flare angle, branches of the curve appear for different flare angles, in this instance 10° and 15° . Each branch for a particular flare angle rises with a slope that continually increases as the length of the flare increases. The successive branch-points from left to right represent greater lengths of the cylinder. Note that for a given flare angle the initial slope of the branch curve is greater for a greater length of the cylinder. These comparisons are for pivot locations that are a constant distance from the nose. The theory predicts, as might be expected, that the effect of a rearward shift of the pivot location is destabilizing. The trends in the test data agree qualitatively with those shown here so long as no extensive flow separation exists. A significant exception is that the test data show the cylinder to contribute to the damping in such a way that each succeeding branch point should be higher on the plot than the one preceding it on the left.

With regard to test techniques, a comparison was made between free and forced oscillation damping data and the results are shown in Figure 16. Forced-oscillation data are shown for a range of amplitude from which the free-oscillation data were obtained. The agreement was as good as the repeatability of the free-oscillation data over the Mach number ranges where the configuration was stable. In the unstable range the free oscillation data were in the form of limit cycle amplitudes. These are compared with the forced-oscillation amplitude of zero damping in Figure 17. The disagreement is attributed, at least in part, to the poor repeatability of the free-oscillation data in the transonic range.

The effects of varying reduced frequency have been investigated in several instances. The forced-oscillation data have shown no effects even though the reduced frequency was varied by a factor greater than two. This was in a range of reduced frequency, $\omega D/2V_\infty$, of 0.004 to 0.020. The free-oscillation data have shown some apparent effects of reduced frequency variation near $M = 1$; however, there were no distinct trends and it is possible that the differences are attributable to uncertainties and poor repeatability in the particular sets of data. It is noted that these reduced frequencies are considerably below the range at which effects would normally be expected.

4. CONCLUSIONS

The following conclusions are made with regard to the aerodynamics of blunted-cone-cylinder-flare configurations:

- (a) A transonic flow separation phenomenon which is characterized by large changes in the pattern of separation with small changes in angle of attack is typical.
- (b) Configurations having combinations of cone angle and flare angle exceeding certain limiting values exhibit dynamic instability in the transonic range.
- (c) Both the static stability and the dynamic stability can be increased by increasing the length of the cylinder and the flare.

- (d) Due to the large effects of flow separation and to the close relationship between the separation patterns and the Reynolds number, it is important that Reynolds number effects be considered in the experimental evaluation of the stability of these configurations.

REFERENCES

1. Gray, J. Don *Boundary-Layer Separation Effects on the Static Stability of a Flared-Tail Missile Configuration at $M = 2$ to 5.* AEDC-TN-60-103, June 1960.
2. Rainey, A. Gerald *Measurement of Aerodynamic Forces for Various Mean Angles of Attack on an Airfoil Oscillating Pitch and on Two Finite-Span Wings Oscillating in Bending with Emphasis on Damping in the Stall.* NACA TN 3643, May 1956.

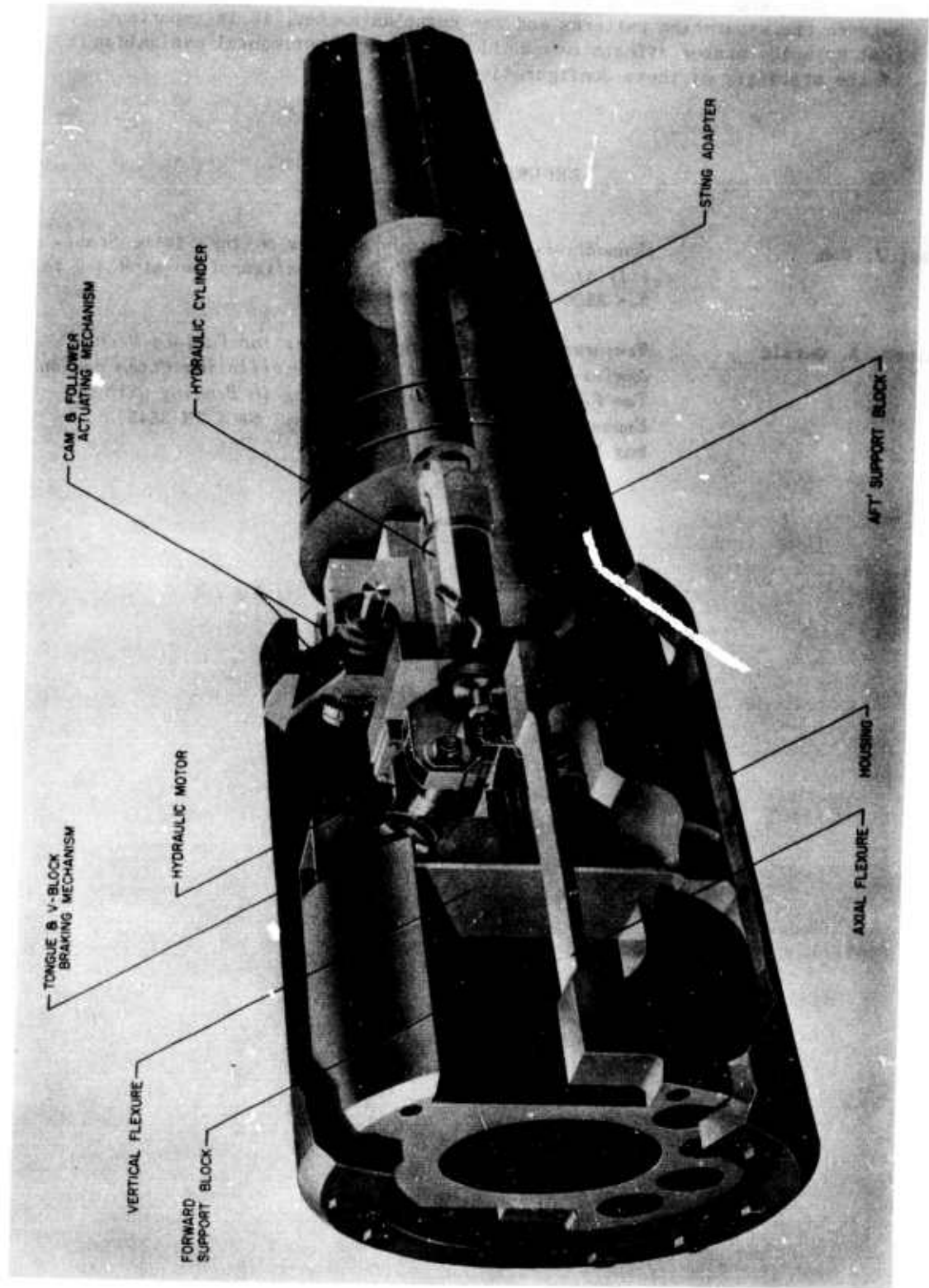


Fig.1 Dynamic support, propulsion wind tunnel

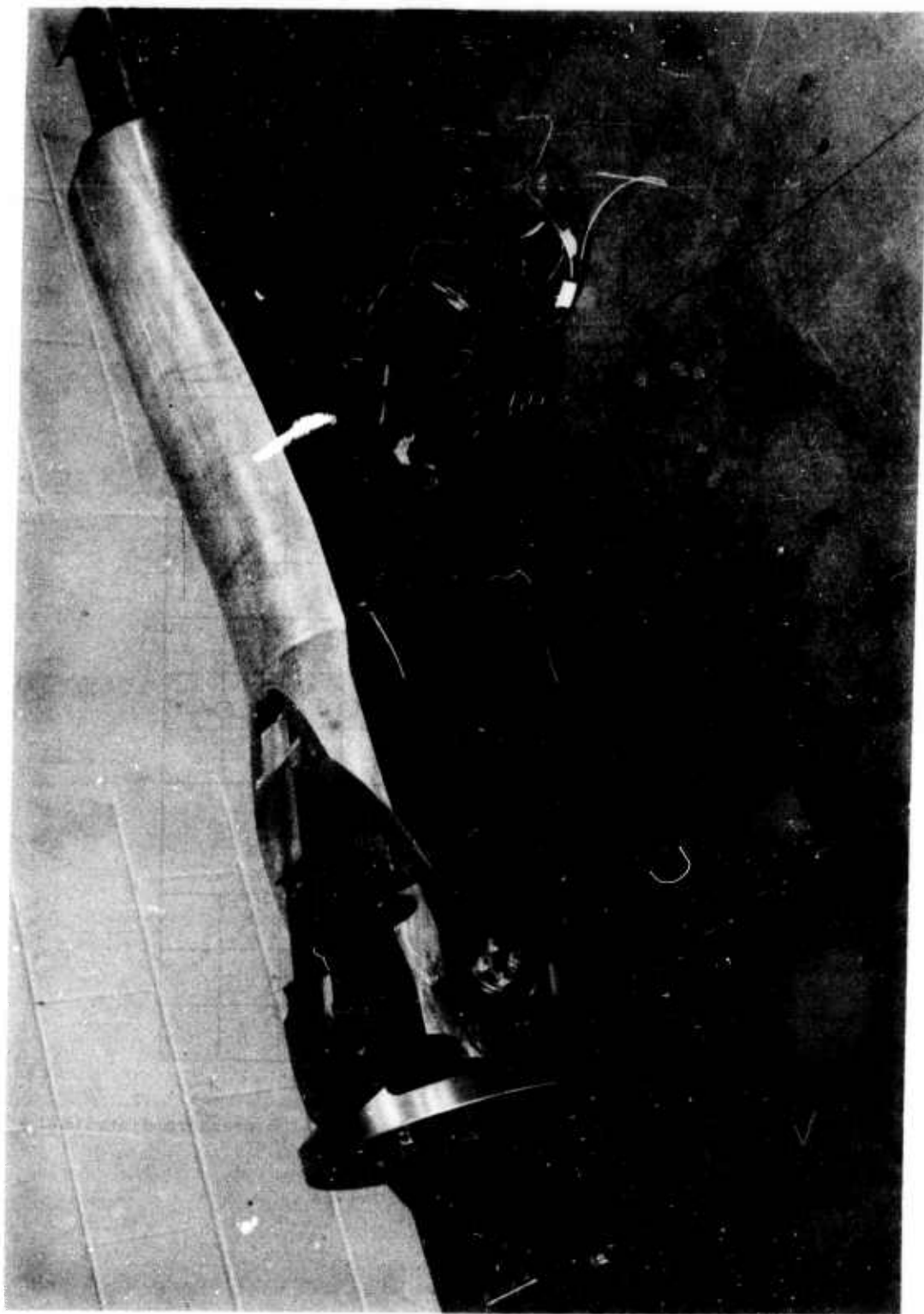


Fig.2 Forced-oscillation balance, propulsion wind tunnel

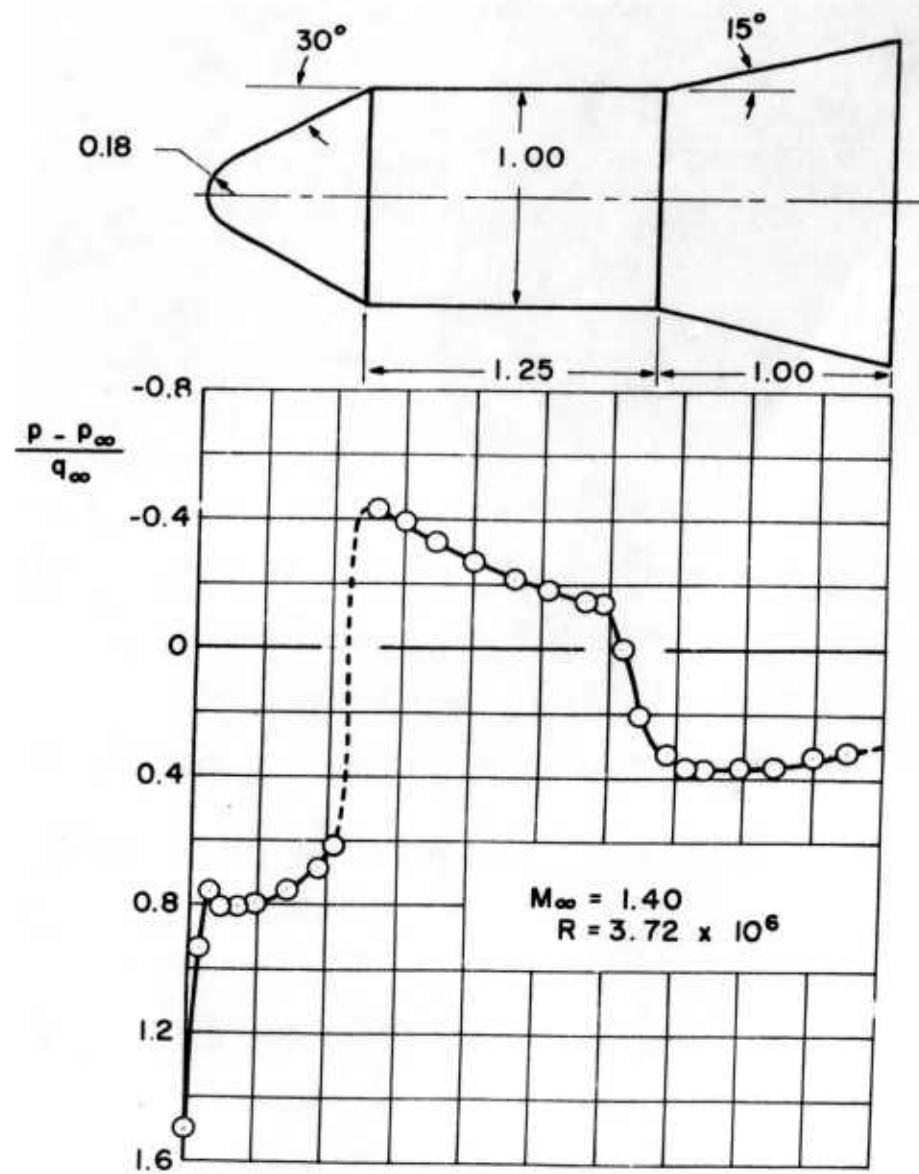


Fig.3 Typical blunted-cone-cylinder-flare configuration with pressure distribution

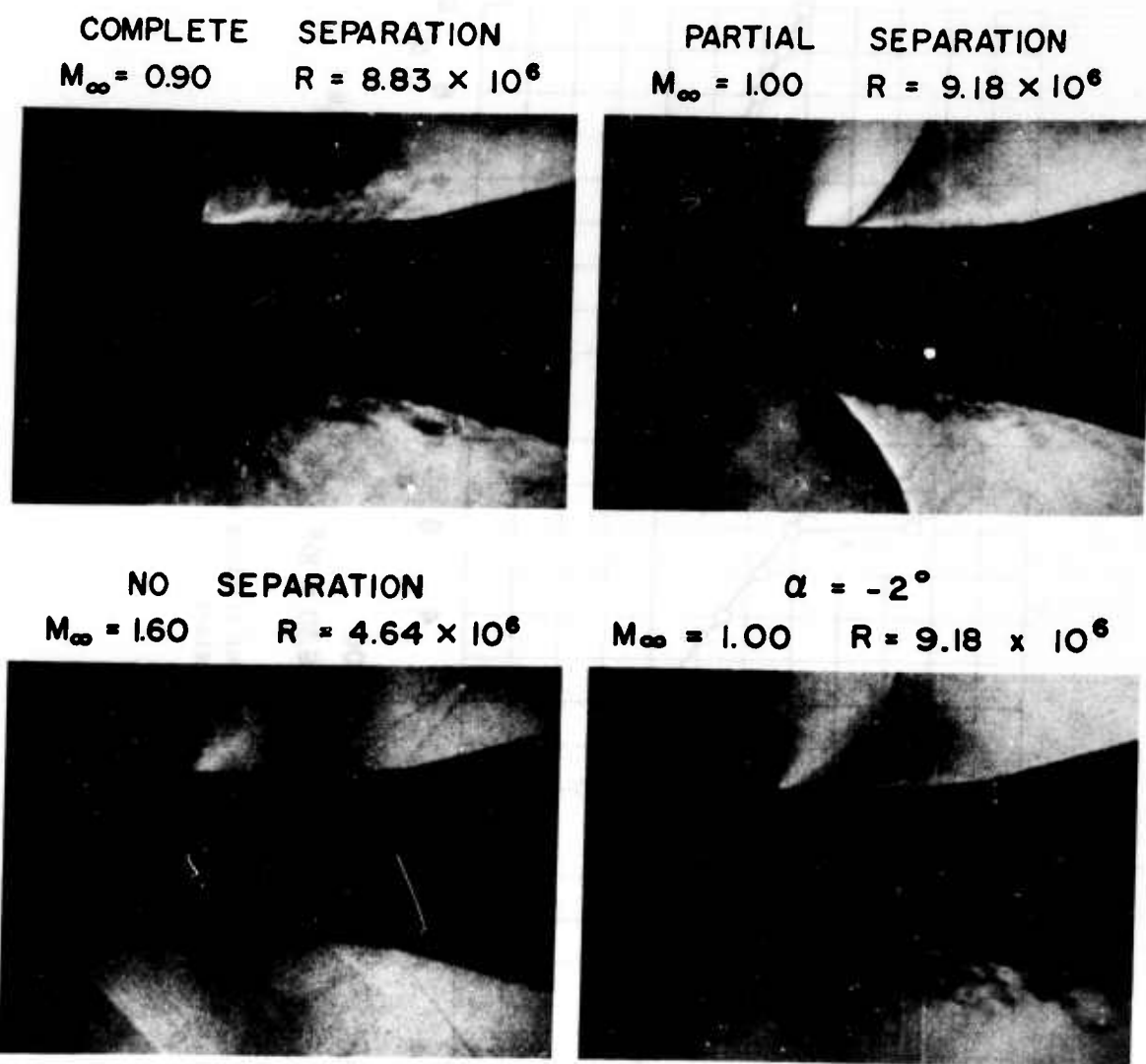


Fig.4 Schlieren photographs of flow field

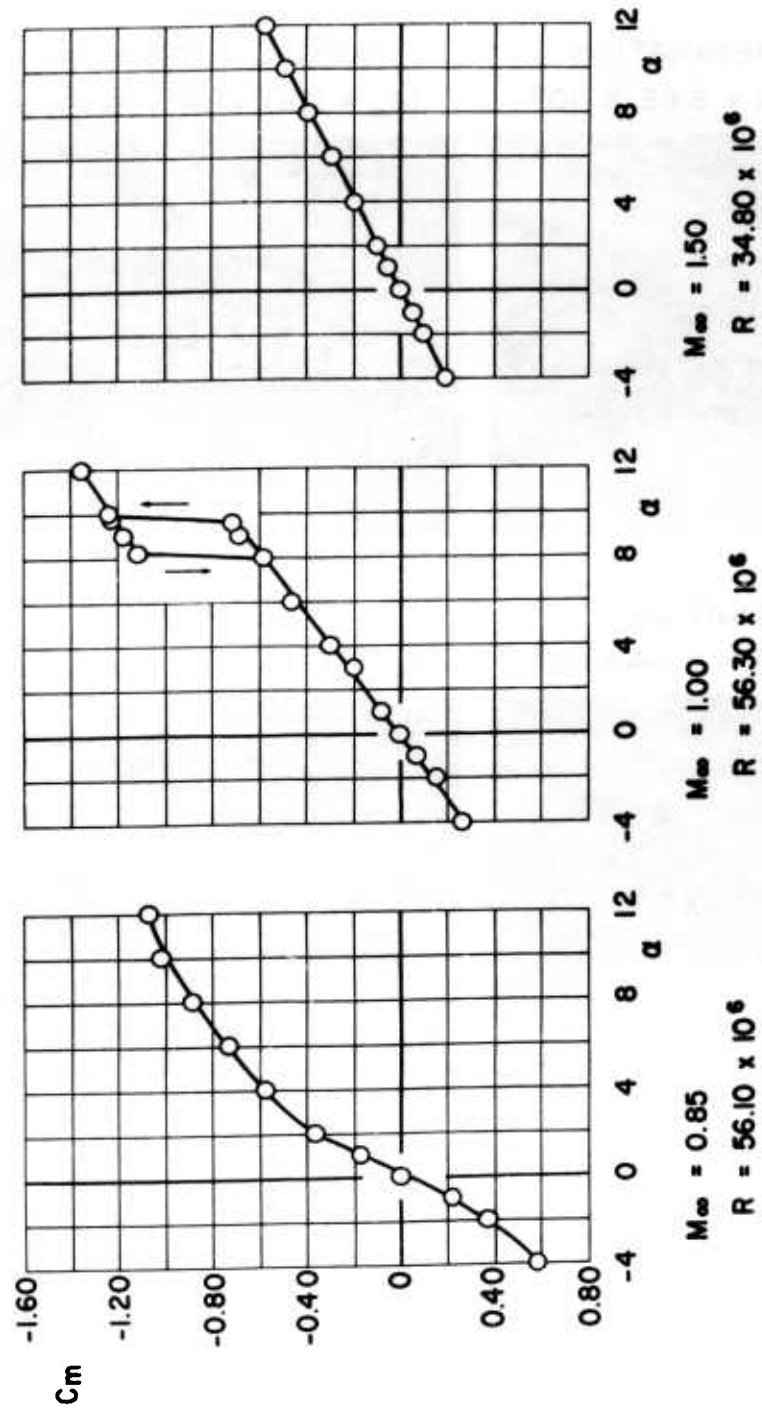
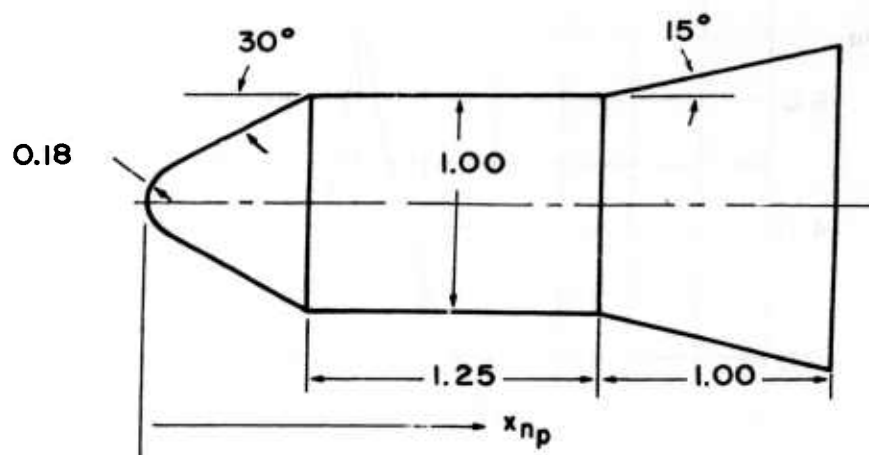


Fig. 5 Effect of Mach number on variation of pitching moment coefficient with angle of attack



○ CLEAN BODY
 □ SURFACE ROUGHNESS ELEMENTS ADDED

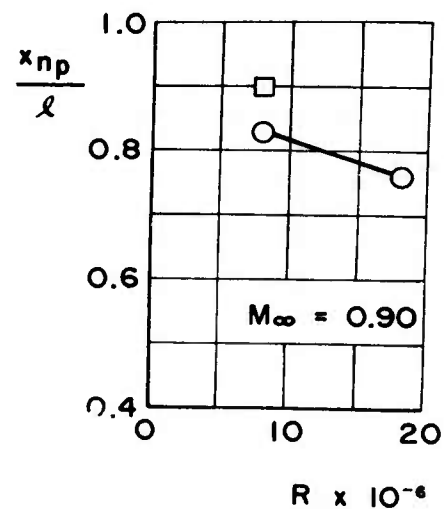
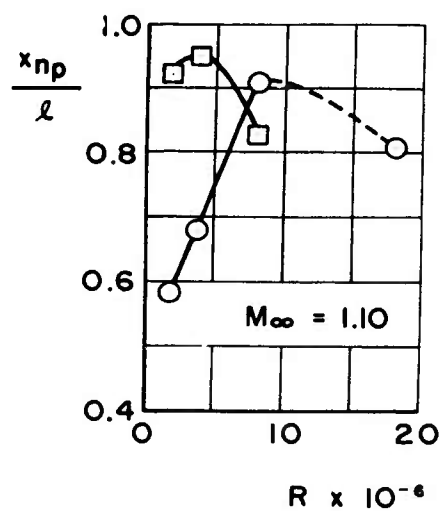


Fig.6 Effect of Reynolds number and surface roughness on neutral point location

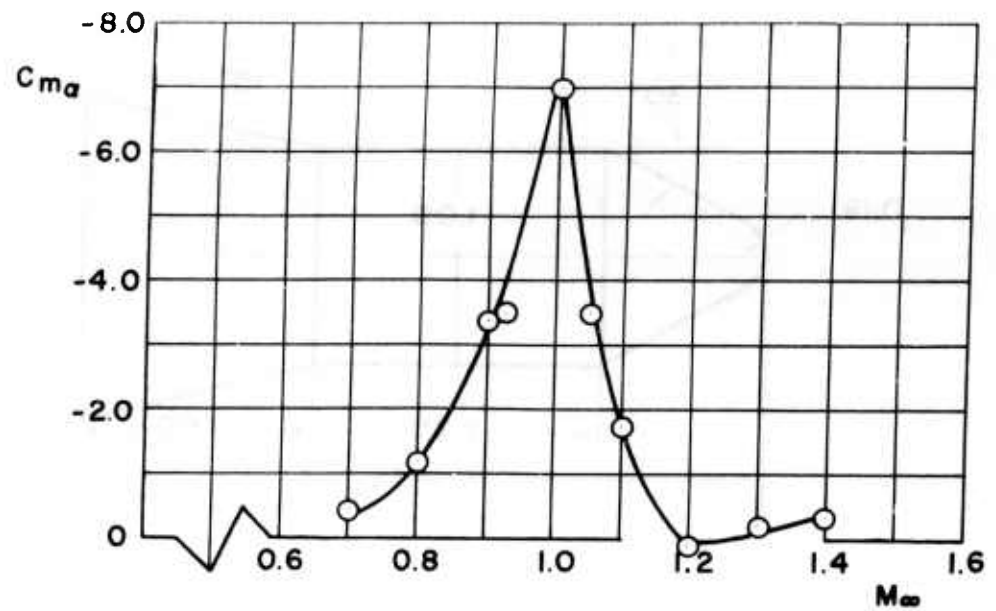


Fig.7 Typical variation of $C_{m\alpha}$ with Mach number

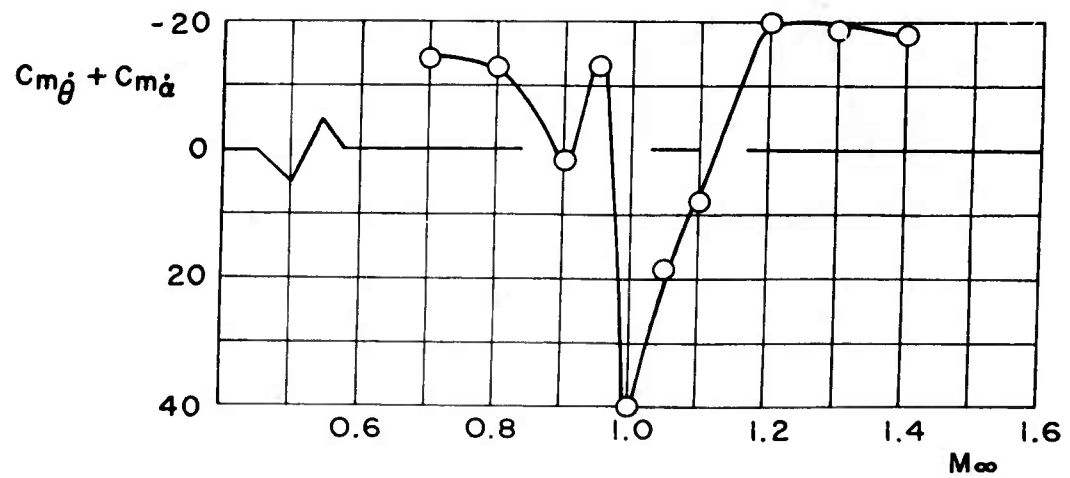


Fig.8 Typical variation of $C_{m\dot{\theta}} + C_{m\dot{\alpha}}$ with Mach number

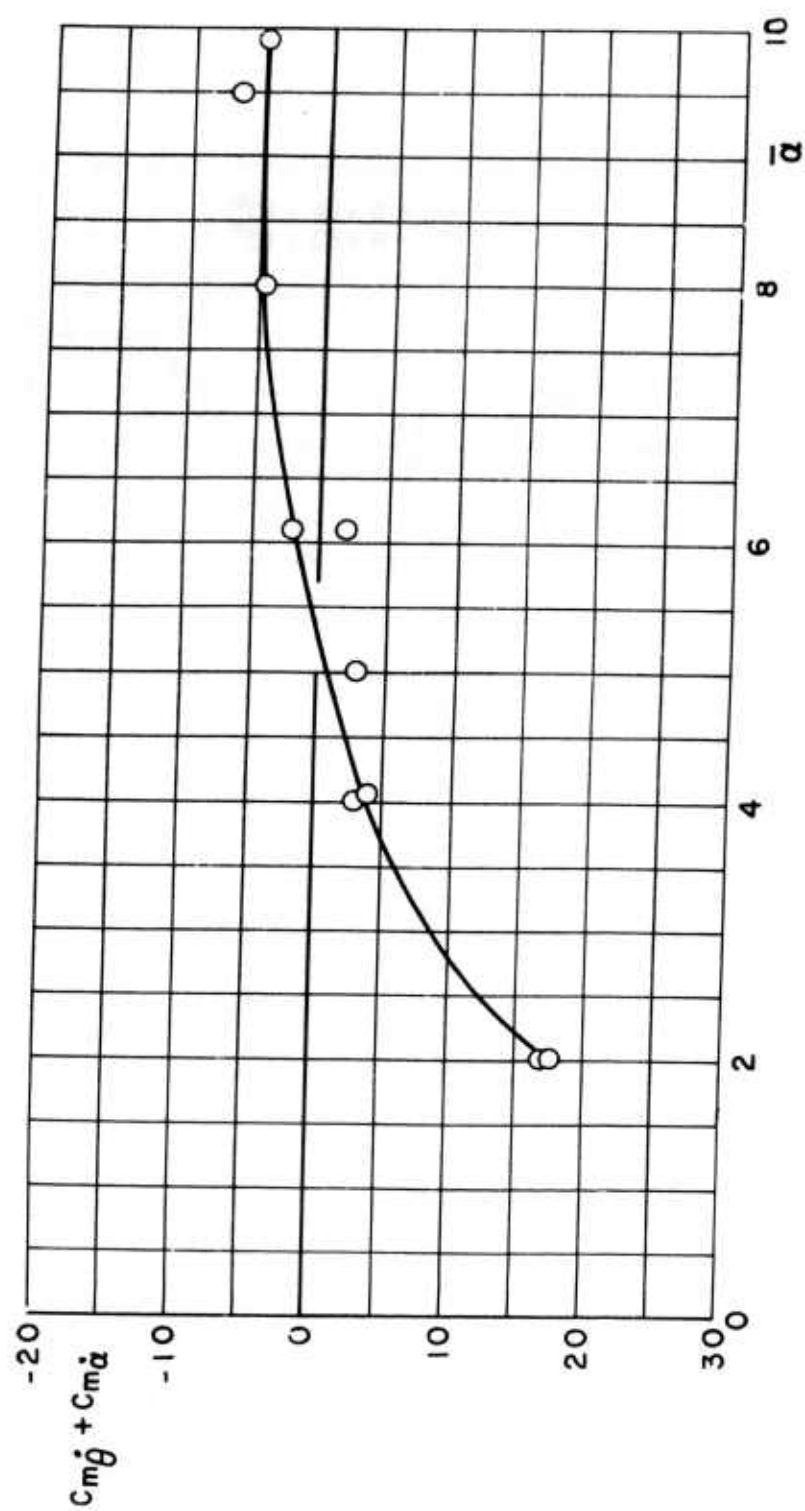


Fig. 9 Effect of oscillation amplitude on $C_m\dot{\theta} + C_m\ddot{\alpha}$

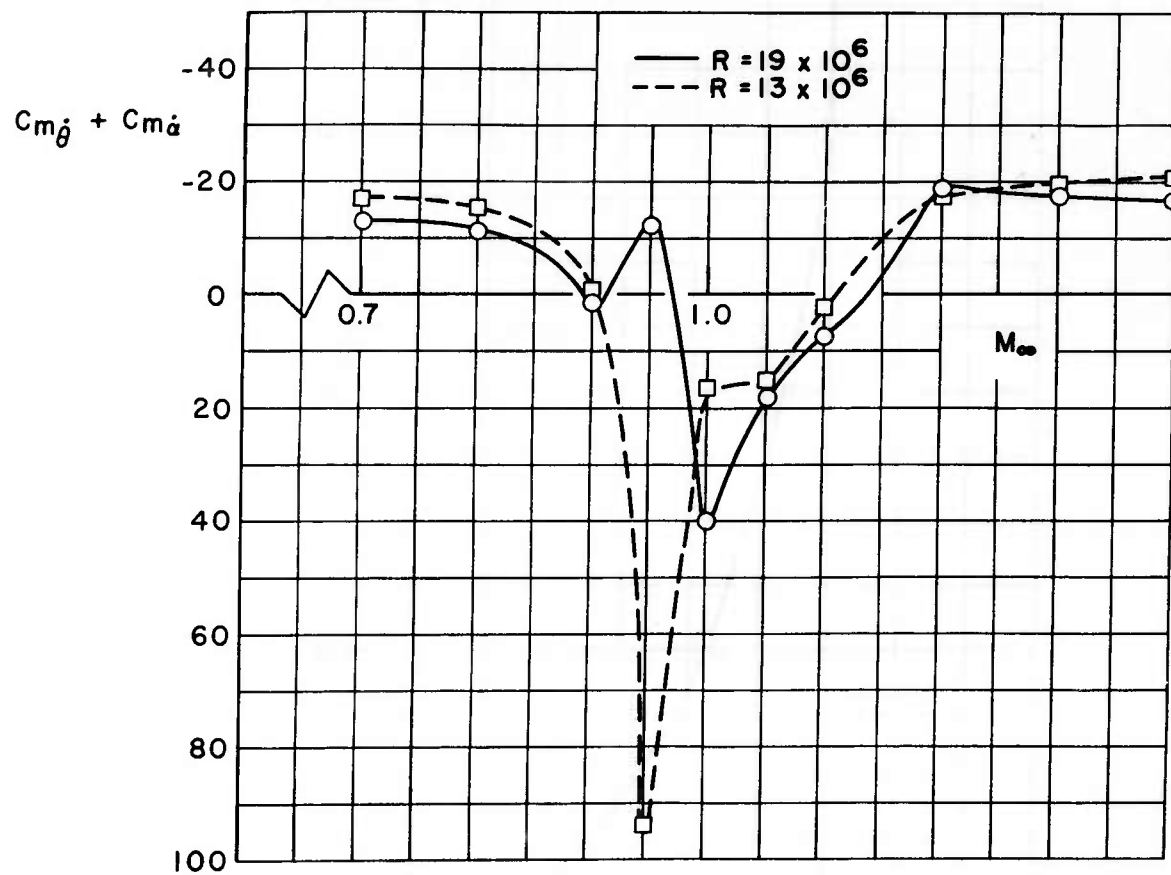


Fig.10 Effect of Reynolds number on variation of $C_{m\dot{\theta}} + C_{m\dot{\alpha}}$ with Mach number

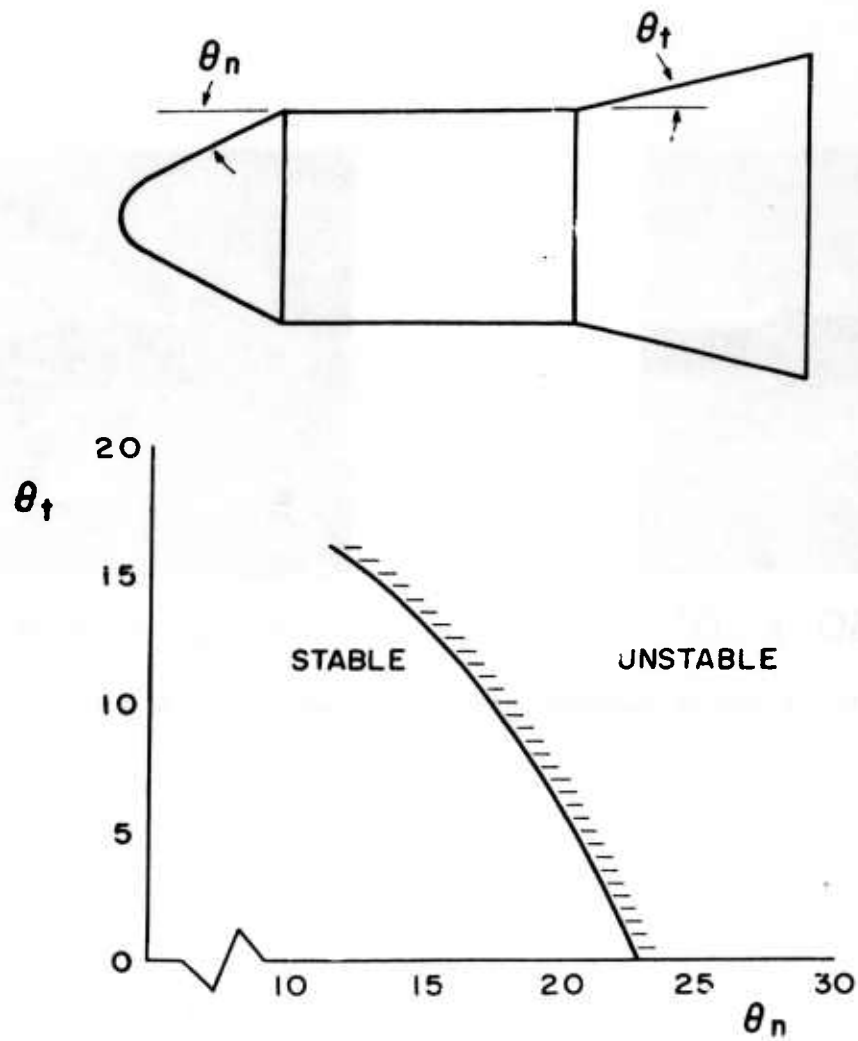
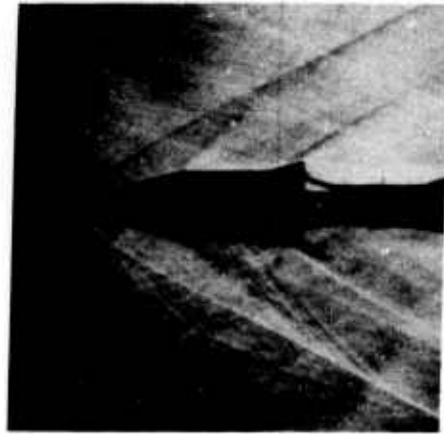


Fig.11 Transonic dynamic stability boundary for typical blunted-cone-cylinder-flare configurations



$$R = 0.50 \times 10^6$$



$$R = 2.10 \times 10^6$$

Fig.12 Effect of Reynolds number on flow pattern at $M_\infty = 2.5$

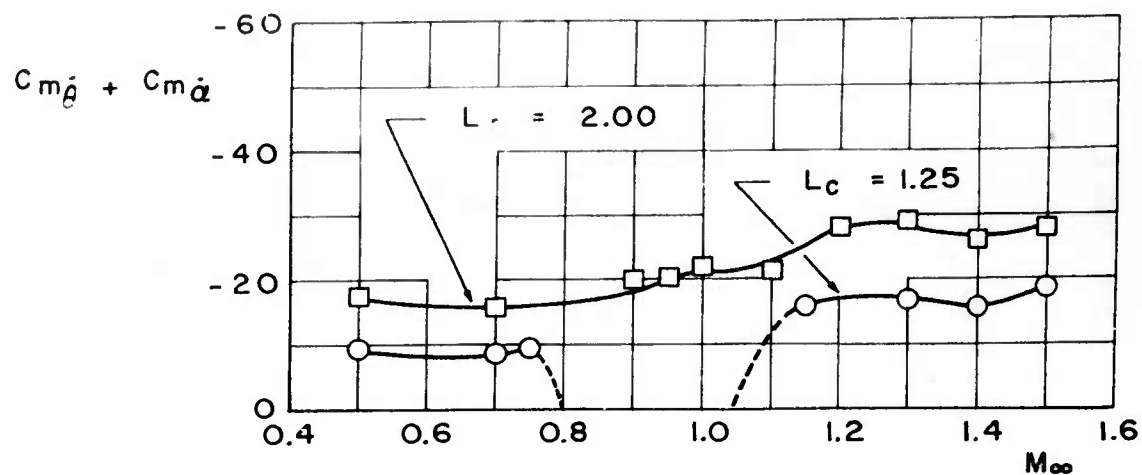


Fig.13 Effect of centerbody length on variation of $C_{m\dot{\theta}} + C_{m\dot{\alpha}}$ with Mach number

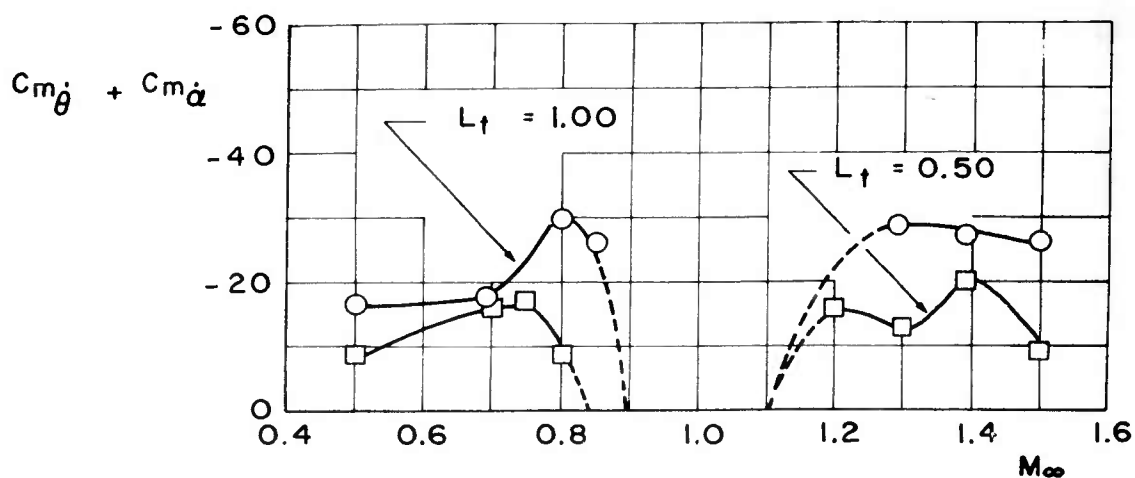


Fig.14 Effect of flare length on variation of $C_{m\dot{\theta}} + C_{m\dot{\alpha}}$ with Mach number

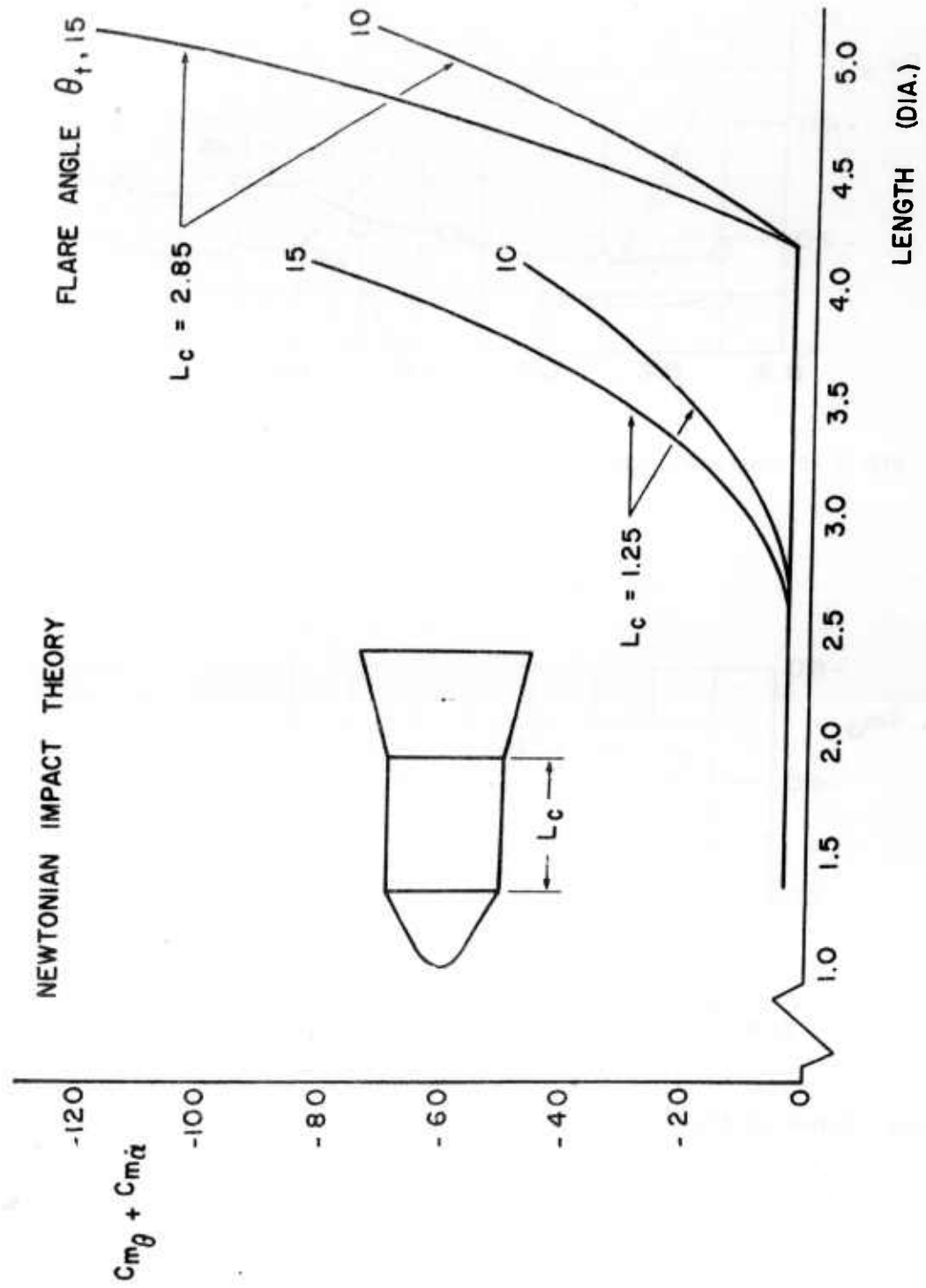


Fig. 15 Variation of $C_{m\dot{\theta}} + C_{m\ddot{\alpha}}$ with body length according to Newtonian impact theory

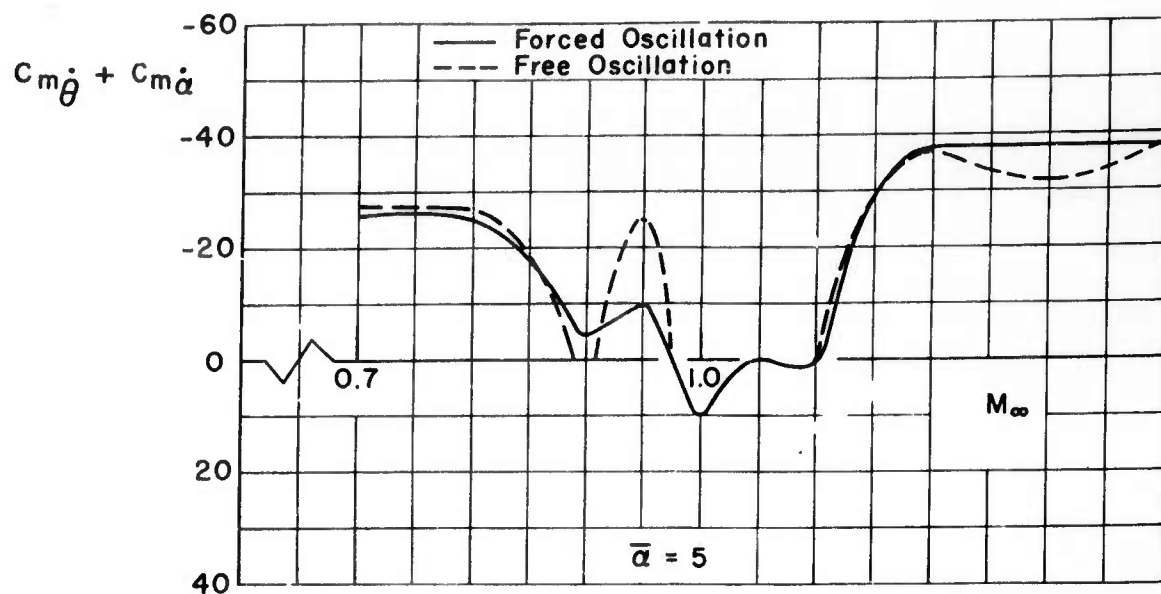


Fig.16 Comparison of $C_{m\dot{\rho}} + C_{m\dot{\alpha}}$ values from free-oscillation and forced-oscillation tests

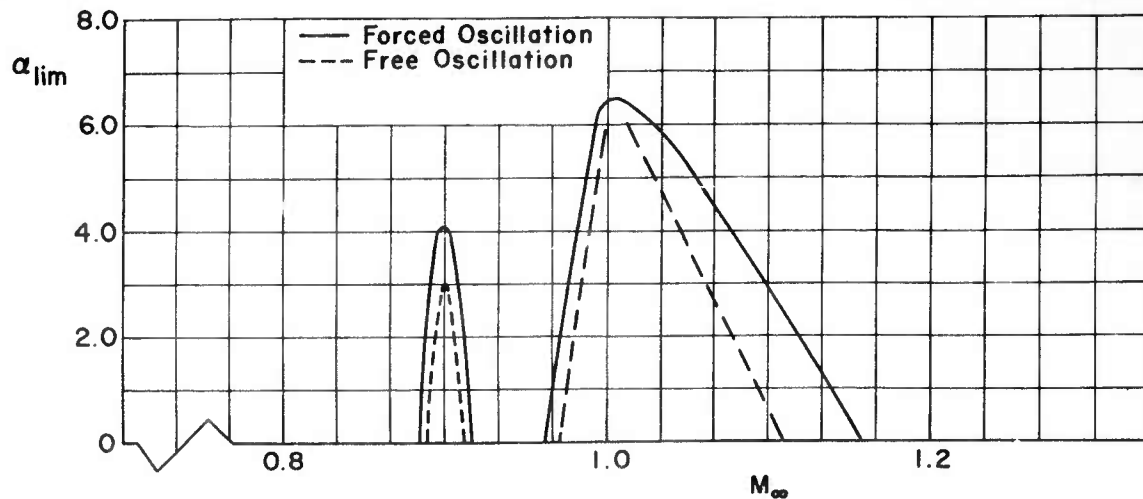


Fig.17 Comparison of limit cycle amplitudes from free-oscillation tests with amplitudes for zero damping from forced-oscillation tests

DISCUSSION

J.C. Wimpenny (U.K.): Your results show three features on which I would like to question you:

- (a) Important Reynolds number effects are continuing up to high values of Reynolds number - at least 19×10^6 .
- (b) At $M_\infty = 1.10$ (Fig. 6) the main effect of increased Reynolds number is to worsen flow separation.
- (c) At $M_\infty = 2.5$ the effect of Reynolds number is to lessen the flow separation.

The fact that significant changes in flow separation are still occurring at high Reynolds number has disturbing implications on the reliability of many transonic and supersonic wind tunnel tests on any wing or body configurations on which flow separations may be encountered, for many routine tests are of necessity done in these ranges of Reynolds number. It is therefore very important to understand the physical process underlying these separations so that one can form the best possible judgment as to their possible full-scale occurrence. It is also disturbing to find two completely opposed trends of Reynolds number effect at two different Mach numbers.

One wonders to what extent two possible flow mechanisms are affecting this, viz., the extents of laminar and turbulent flow, and the fundamental thinning of a turbulent boundary layer as Reynolds number is increased. I would be grateful for any comments you may have on these questions.

Author's reply: Our work to date on this has been limited to measurement of static pressure distributions, forces and moments, and longitudinal dynamic stability. In other words, we have not yet explored the boundary layers. However, the following comments are offered in regard to the items which you enumerate.

- (a) The flow separation with which we are mostly concerned occurs near the nose of the model. Therefore, my use of Reynolds number based on model length may have been somewhat misleading. Also, another phenomenon may be further reducing the effective Reynolds number. I am referring to the inverse transition which Sternberg* has observed on cone-cylinders. He reports cases in which a turbulent boundary layer on the cone is more or less dissipated at the cone cylinder junction, where a new laminar boundary layer begins. The new laminar layer is then capable of undergoing transition to a turbulent layer, or presumably it might separate in accordance with the usual characteristics of laminar boundary layers. We have no evidence, however, that this is or is not happening in our tests.
- (b),(c) The separation at $M_\infty = 2.5$ seems to depend primarily on the flare and only to a much lesser extent on the cone for the configurations we have tested.

*Sternberg, Joseph, *The Transition from a Turbulent to a Laminar Boundary Layer*. Ballistic Research Laboratories Report 906, 1954.

The $M_\infty = 1.1$ separation, however, is strongly influenced by the adverse pressure gradient immediately aft of the cone-cylinder junction as well as by the pressure rise due to the flare. Although this does not in itself explain the differences in trends with increasing Reynolds number at these two Mach numbers, it does at least indicate that two different mechanisms are involved.

With regard to the transonic case, I might add, although I am not sure of its applicability in our case, that Pearcey* reports shock-induced separation effects increasing when the boundary layer transition moves from a position downstream of the separation point to a position upstream of the separation. Pearcey's report deals with wings, rather than bodies of revolution, and the separation effects were measured by the decrease in pressure recovery at the trailing edge.

B. Etkin (Canada): I have two rather minor points to raise with Mr. DuBose.

- (1) Is it possible that there has been a mistake in sign in the point on Figures 8 and 10 which occurs at $M = 0.95$? It would be much more believable if it were positive instead of negative.
- (2) I wonder whether a different notation for damping should be used when we are dealing with non-linear (amplitude-dependent) aerodynamic forces, as in Figure 9, $C_{m\dot{\theta}}$ and $C_{m\dot{\alpha}}$ are ordinarily defined as (constant) coefficients of proportionality for a linear case, or as the slopes of local tangents otherwise. In the present instance, I take it that the definition of $(C_{m\dot{\alpha}} + C_{m\dot{\theta}})$ is based on average energy dissipation over a cycle, but then the symbols themselves lose completely the meanings implied, viz.:

$$C_{m\dot{\alpha}} = \partial C_m / \left(\partial \frac{\dot{\alpha}_1}{U} \right)$$

Author's reply: My thanks to Mr. Etkin for his comments. With regard to his first question, the data point was very definitely established by the forced oscillation technique and also checked qualitatively by the free-oscillation technique. With regard to the second question, the damping coefficient, as used here, was an effective linear value corresponding to the fundamental content of the angular displacement and the out-phase moment averaged over a number of cycles. Perhaps some other notation would be more meaningful.

K. Orlik-Rückemann (Canada): We have completed recently a series of measurements on oscillating blunt bodies of revolution, and I happen to have with me three slides with some of the results. During the lecture I was comparing these results with those presented by Mr. DuBose and it appears that the general agreement (in trends) is very good even if the configurations tested and the experimental techniques used were quite different. I am going to show you these three slides as I think that they will support

*Pearcey, H.H., *A Method for the Prediction of the Onset of Buffeting and Other Separation Effects from Wind Tunnel Tests on Rigid Models*. NPL/Aero/358.

Mr. DuBose's results. I hope that you do not think that I am taking an unfair advantage of being your chairman to force on you one extra lecture! I will be as concise as possible.

The experiments were made in the NAE 30 inch suction wind tunnel, using half models and our standard technique of free oscillations with feedback excitation. The configurations tested consisted of a cylinder, a hemisphere-cylinder, and two hemisphere-cylinder-flare combinations, as shown on the first slide (Fig. A-1), on which also the axis of oscillation is indicated. The notation $C_{m\dot{\theta}}$ is equivalent to $(C_{m\dot{\theta}} + C_{m\dot{\alpha}})$ as used by Mr. DuBose. We see that the subsonic dynamic instability of a cylinder disappears when a hemisphere is attached to its front. An increase of the flare angle from initial 0° (no flare) produces at transonic speeds a distinct peak of reduced dynamic stability, which at flare angle 20° is completely unstable. Note the number of points describing the peak in this last case which, I think, also shows a high accuracy of data. From the comparison of data obtained with the model mounted on the reflection plate (in the free stream) and directly on the wall, the effect of tunnel wall boundary layer can be obtained. It seems to reduce greatly the height of the transonic peak and also to displace it somewhat towards a higher Mach number. The Reynolds number of the tests, based on cylinder diameter, was close to 1 million in the transonic range.

The second slide (Fig. A.2) shows corresponding data on the aerodynamic stiffness derivative $C_{m\theta}$. The last slide (Fig. A.3) shows the effect of flare angle on the peak value of the transonic damping reduction and the corresponding values of $C_{m\theta}$. For the present axis of oscillation it can be seen that a narrow range of flare angle ($9^\circ - 12^\circ$) exists, for which both derivatives are in the 'stable' region throughout the Mach number range investigated.

The data are given in terms of flare angle but, of course, can just as well be presented as a function of base area, as the two quantities are related by the flare length, which is constant.

The investigation is described by Mr. K.G. LaBerge in NAE Report LR 295, which will be shortly available.

O.E. Michaelsen (Canada): With regard to the effect of Reynolds' number on damping as shown in Figure 10, it appears that there are only two test points that disagree by a large amount. I would like to question Mr. DuBose on how sure he is that the test points in question are correct, or in other words, have repeat measurements confirmed this difference?

Author's reply: In response to Mr. Michaelsen's question, I am quite sure that the points are correct. These data are very typical of our experience with strong Reynolds number effects on both the static and dynamic stability of many blunted-cone-cylinder-flare type models at transonic speeds. However, as Mr. Orlik-Rückemann has pointed out to me, perhaps the way the points are faired is quite arbitrary.

A.W. Babister (U.K.): How far are the marked scale effects and irregular damping at transonic speeds bound up with the sharp corner on your models? Mr. Orlik-Rückemann's

figures (on hemisphere-cylinder models) do not appear to show such irregular transonic effects.

Author's reply: The sharp corner is, in my opinion, important in that respect. Generally, the radius of curvature of the corner is about 2 or 3% of the centerbody diameter. In one case where the radius of curvature was increased considerably, I believe the variation of the damping coefficient was considerably less, but the instability was still there.

L.C. Macallister (U.S.A.): With regard to the previous questions on Reynolds number effects indicated in the data and their reliability, I believe I recognize the data and, if so, free-flight data from several installations and at several Reynolds numbers were consistent with the Reynolds number effect shown and the two types of tests were in substantial agreement.

ADDENDUM

AGARD SPECIALISTS' MEETING

on

STABILITY AND CONTROL

Complete List of Papers Presented

Following is a list of the titles and authors of the 41 papers presented at the Stability and Control Meeting held in Brussels in April, 1960, together with the AGARD Report number covering the publication of each paper.

INTRODUCTORY PAPERS

The Aeroplane Designer's Approach to Stability and Control, by
G.H.Lee (United Kingdom) Report 334

The Missile Designer's Approach to Stability and Control Problems, by
M.W.Hunter and J.W.Hindes (United States) Report 335

DESIGN REQUIREMENTS

Flying Qualities Requirements for United States Navy and Air Force Aircraft, by W.Koven and R.Wasicko (United States) Report 336

Design Aims for Stability and Control of Piloted Aircraft, by
H.J.Allwright (United Kingdom) Report 337

Design Criteria for Missiles, by L.G.Evans (United Kingdom) Report 338

AERODYNAMIC DERIVATIVES

State of the Art of Estimation of Derivatives, by H.H.B.M.Thomas
(United Kingdom) Report 339

The Estimation of Oscillatory Wing and Control Derivatives, by
W.E.A.Acum and H.C.Garner (United Kingdom) Report 340

Current Progress in the Estimation of Stability Derivatives, by
L.V.Malthan and D.E.Hoak (United States) Report 341

Calculation of Non-Linear Aerodynamic Stability Derivatives of Aeroplanes, by K.Gersten (Germany) Report 342

<i>Estimation of Rotary Stability Derivatives at Subsonic and Transonic Speeds</i> , by M.Tobak and H.C.Lessing (United States)	Report 343
<i>Calcul par Analogie Rhéoelectrique des Dérivées Aérodynamiques d'une Aile d'Envergure Finie</i> , by M.Enselme and M.O.Aguesse (France) ..	Report 344
<i>A Method of Accurately Measuring Dynamic Stability Derivatives in Transonic and Supersonic Wind Tunnels</i> , by H.G.Wiley and A.L.Braslow (United States)	Report 345
<i>Mesure des Dérivées Aérodynamiques en Soufflerie et en Vol</i> , by M.Scherer and P.Mathe (France)	Report 346
<i>Static and Dynamic Stability of Blunt Bodies</i> , by H.C.DuBose (United States)	Report 347

AEROELASTIC EFFECTS

<i>Effects of Aeroelasticity on the Stability and Control Characteristics of Airplanes</i> , by H.L.Runyan, K.G.Pratt and F.V.Bennett (United States)	Report 348
<i>The Influence of Structural Elasticity on the Stability of Airplanes and Multistage Missiles</i> , by L.T.Prince (United States)	Report 349
<i>Discussion de deux Méthodes d'Etude d'un Mouvement d'un Missile Flexible</i> , by M.Bismut and C.Beatrix (France)	Report 350
<i>The Influence of Aeroelasticity on the Longitudinal Stability of a Swept-Wing Subsonic Transport</i> , by C.M.Kalkman (Netherlands)	Report 351
<i>Some Static Aeroelastic Considerations of Slender Aircraft</i> , by G.J.Hancock (United Kingdom)	Report 352

COUPLING PHENOMENA

<i>Pitch-Yaw-Roll Coupling</i> , by L.L.Cronvich and B.E.Amsler (United States)	Report 353
<i>Application du Calculateur Analogique à l'Etude du Couplage des Mouvements Longitudinaux et Transversaux d'un Avion</i> , by F.C.Haus (Belgium)	Report 354
<i>Influence of Deflection of the Control Surfaces on the Free-Flight Behaviour of an Aeroplane: A Contribution to Non-Linear Stability Theory</i> , by X.Hafer (Germany)	Report 355

STABILITY AND CONTROL AT HIGH LIFT

<i>Low-Speed Stalling Characteristics</i> , by J.C.Wimpenny (United Kingdom)	Report 356
--	------------

<i>Some Low-Speed Problems of High-Speed Aircraft</i> , by A.Spence and D.Lean (United Kingdom)	Report 357
<i>Factors Limiting the Landing Approach Speed of an Airplane from the Viewpoint of a Pilot</i> , by R.C.Innis (United States)	Report 358
<i>Post-Stall Gyration and Their Study on a Digital Computer</i> , by S.H.Scher (United States)	Report 359

THE APPLICATION OF SERVO-MECHANISMS

<i>The Place of Servo-Mechanisms in the Design of Aircraft with Good Flight Characteristics</i> , by K.H.Doetsch (United Kingdom)	Report 360
<i>Effects of Servo-Mechanism Characteristics on Aircraft Stability and Control</i> , by F.A.Gaynor (United States)	Report 361
<i>Les Commandes de Vol Considérées comme Formant un Système Asservi</i> , by J.Grémont (France)	Report 362
<i>Determination of Suitable Aircraft Response as Produced by Automatic Control Mechanisms</i> , by E.Mewes (Germany)	Report 363
<i>An Approach to the Control of Statically Unstable Manned Flight Vehicles</i> , by M.Dublin (United States)	Report 364

THE USE OF SIMULATORS

<i>The Use of Piloted Flight Simulators in General Research</i> , by G.A.Rathert, Jr., B.Y.Creer and M.Sadoff (United States)	Report 365
<i>Simulation in Modern Aero-Space Vehicle Design</i> , by C.B.Westbrook (United States)	Report 366
<i>Mathematical Models for Missiles</i> , by W.S.Brown and D.I.Paddison (United Kingdom)	Report 367
<i>In-Flight Simulation - Theory and Application</i> , by E.A.Kidd, G.Bull and R.P.Harper, Jr. (United States)	Report 368

DEVELOPMENT TECHNIQUES

<i>Application of Analytical Techniques to Flight Evaluations in Critical Control Areas</i> , by J.Weil (United States)	Report 369
<i>Investigation on the Improvement of Longitudinal Stability of a Jet Aircraft by the Use of a Pitch-Damper</i> , by R.Mautino (Italy)	Report 370

Méthodes Utilisées pour la Mise au Point de l'Avion Bréguet 940 à Ailes Soufflées, by G. de Richemont (France) **Report 371**

TURBULENCE AND RANDOM DISTURBANCES

Theory of the Flight of Airplanes in Isotropic Turbulence; Review and Extension, by B.Etkin (Canada) **Report 372**

The Possible Effects of Atmospheric Turbulence on the Design of Aircraft Control Systems, by J.K.Zbrozek (United Kingdom) **Report 373**

L'Optimisation Statistique du Guidage par Alignement d'un Engin Autopropulsé en Présence de Bruit, by P.LeFèvre (France) **Report 374**

ADVISORY GROUP FOR AERONAUTICAL RESEARCH AND DEVELOPMENT
Organisation du Traité de l'Atlantique Nord
64, rue de Varenne — Paris 7^{eme}

August 1961

AGARD Distribution List

Category II: "Not for Sale" Publications

COUNTRY	ADDRESS	NO. OF COPIES
BELGIUM	Centre National d'Etudes et de Recherches Aéronautiques 11, rue d'Egmont, Bruxelles	25
CANADA	T.I.L.—Ministry of Aviation Leysdown Road Mottingham London, S.E.9 Attn: Mr. F. G. Waite	30
DENMARK	Danish Defence Research Board Østerbrogades Kaserne Copenhagen Ø	10
FRANCE	ONERA (Direction) 25, avenue de la Division Leclerc Châtillon-sous-Bagneux, (Seine)	90
GERMANY	Deutsche Gesellschaft für Flugwissen- schaften Zentralstelle für Luftfahrt-dokumenta- tion und Information München 64, Flughafen Attn: Dr. H. J. Rautenberg	90
GREECE	Greek Nat. Def. Gen. Staff B. MEO Athens	10
ICELAND	Director of Aviation c/o Flugrad Reykjavik	3
ITALY	Ufficio del Generale Ispettore del Genio Aeronautico Ministero Difesa-Aeronautica Roma	85
LUXEMBOURG	obtainable through Belgium	

NETHERLANDS	Netherlands Delegation to AGARD Michiel de Ruyterweg, 10 Delft	35*
NORWAY	Norway Defence Research Establishment Kjeller per Lillestrom Attn: Mr. O. Blichner	22
PORTUGAL	Direccao de Servico de Material da Forca Aerea Rua da Escola Politecnica, 42 Lisboa Attn: Coronel Joao A. de Almeida Viana	5
TURKEY	Ministry of National Defence Ankara Attn: AGARD National Delegate	30
UNITED KINGDOM	T.I.L. Ministry of Aviation Leysdown Road Mottingham London, S.E.9 Attn: Mr. F. G. Waite	120
UNITED STATES	National Aeronautics and Space Administration Langley Research Center Langley Field, Virginia Attn: Report Distribution and Storage Unit	400
AGARD	64, rue de Varenne Paris 7 eme	45

*Netherlands meets demands of SHAPE Air Defence Technical Centre.

<p>AGARD Report 347 North Atlantic Treaty Organization, Advisory Group for Aeronautical Research and Development STATIC AND DYNAMIC STABILITY OF BLUNT BODIES H.C. DuBose 1961 27 pages, incl. 2 refs., 17 figs; plus discussion and bibliography of papers presented at the Stability and Control Meeting</p> <p>A description is given of the relationships between the flow fields and the static and dynamic stability of blunted-cone-cylinder-flare-type re-entry bodies at Mach numbers from 0.7 to 5.0. Effects of variations in some of the shape parameters on the dynamic stability are presented. It is shown that certain combinations of cone and flare angles result in instability in the transonic range. Also, comparison is made between free and forced oscillation data.</p> <p>P.T.O.</p>	<p>533.6.013.4 533.696 3c6e7 3b3g2</p>	<p>AGARD Report 347 North Atlantic Treaty Organization, Advisory Group for Aeronautical Research and Development STATIC AND DYNAMIC STABILITY OF BLUNT BODIES H.C. DuBose 1961 27 pages, incl. 2 refs., 17 figs; plus discussion and bibliography of papers presented at the Stability and Control Meeting</p> <p>A description is given of the relationships between the flow fields and the static and dynamic stability of blunted-cone-cylinder-flare-type re-entry bodies at Mach numbers from 0.7 to 5.0. Effects of variations in some of the shape parameters on the dynamic stability are presented. It is shown that certain combinations of cone and flare angles result in instability in the transonic range. Also, comparison is made between free and forced oscillation data.</p> <p>P.T.O.</p>	<p>533.6.013.4 533.696 3c6e7 3b3g2</p>
<p>AGARD Report 347 North Atlantic Treaty Organization, Advisory Group for Aeronautical Research and Development STATIC AND DYNAMIC STABILITY OF BLUNT BODIES H.C. DuBose 1961 27 pages, incl. 2 refs., 17 figs; plus discussion and bibliography of papers presented at the Stability and Control Meeting</p> <p>A description is given of the relationships between the flow fields and the static and dynamic stability of blunted-cone-cylinder-flare-type re-entry bodies at Mach numbers from 0.7 to 5.0. Effects of variations in some of the shape parameters on the dynamic stability are presented. It is shown that certain combinations of cone and flare angles result in instability in the transonic range. Also, comparison is made between free and forced oscillation data.</p> <p>P.T.O.</p>	<p>533.6.013.4 533.696 3c6e7 3b3g2</p>	<p>AGARD Report 347 North Atlantic Treaty Organization, Advisory Group for Aeronautical Research and Development STATIC AND DYNAMIC STABILITY OF BLUNT BODIES H.C. DuBose 1961 27 pages, incl. 2 refs., 17 figs; plus discussion and bibliography of papers presented at the Stability and Control Meeting</p> <p>A description is given of the relationships between the flow fields and the static and dynamic stability of blunted-cone-cylinder-flare-type re-entry bodies at Mach numbers from 0.7 to 5.0. Effects of variations in some of the shape parameters on the dynamic stability are presented. It is shown that certain combinations of cone and flare angles result in instability in the transonic range. Also, comparison is made between free and forced oscillation data.</p> <p>P.T.O.</p>	<p>533.6.013.4 533.696 3c6e7 3b3g2</p>

This Report is one in the Series 334-374, inclusive, presenting papers, with discussions, given at the AGARD Specialists' Meeting on 'Stability and Control', Training Center for Experimental Aerodynamics, Rhode-Saint-Genèse, Belgium, 10-14 April 1961, sponsored jointly by the AGARD Fluid Dynamics and Flight Mechanics Panels

This Report is one in the Series 334-374, inclusive, presenting papers, with discussions, given at the AGARD Specialists' Meeting on 'Stability and Control', Training Center for Experimental Aerodynamics, Rhode-Saint-Genèse, Belgium, 10-14 April 1961, sponsored jointly by the AGARD Fluid Dynamics and Flight Mechanics Panels

This Report is one in the Series 334-374, inclusive, presenting papers, with discussions, given at the AGARD Specialists' Meeting on 'Stability and Control', Training Center for Experimental Aerodynamics, Rhode-Saint-Genèse, Belgium, 10-14 April 1961, sponsored jointly by the AGARD Fluid Dynamics and Flight Mechanics Panels

This Report is one in the Series 334-374, inclusive, presenting papers, with discussions, given at the AGARD Specialists' Meeting on 'Stability and Control', Training Center for Experimental Aerodynamics, Rhode-Saint-Genèse, Belgium, 10-14 April 1961, sponsored jointly by the AGARD Fluid Dynamics and Flight Mechanics Panels

<p>AGARD Report 347 North Atlantic Treaty Organization, Advisory Group for Aeronautical Research and Development STATIC AND DYNAMIC STABILITY OF BLUNT BODIES H.C. DuBose 1961 27 pages, incl. 2 refs., 17 figs; plus discussion and bibliography of papers presented at the Stability and Control Meeting</p> <p>A description is given of the relationships between the flow fields and the static and dynamic stability of blunted-cone-cylinder-flare-type re-entry bodies at Mach numbers from 0.7 to 5.0. Effects of variations in some of the shape parameters on the dynamic stability are presented. It is shown that certain combinations of cone and flare angles result in instability in the transonic range. Also, comparison is made between free and forced oscillation data.</p> <p>P.T.O.</p>	<p>533.6.013.4 533.696 3c6e7 3b3g2</p>	<p>AGARD Report 347 North Atlantic Treaty Organization, Advisory Group for Aeronautical Research and Development STATIC AND DYNAMIC STABILITY OF BLUNT BODIES H.C. DuBose 1961 27 pages, incl. 2 refs., 17 figs; plus discussion and bibliography of papers presented at the Stability and Control Meeting</p> <p>A description is given of the relationships between the flow fields and the static and dynamic stability of blunted-cone-cylinder-flare-type re-entry bodies at Mach numbers from 0.7 to 5.0. Effects of variations in some of the shape parameters on the dynamic stability are presented. It is shown that certain combinations of cone and flare angles result in instability in the transonic range. Also, comparison is made between free and forced oscillation data.</p> <p>P.T.O.</p>	<p>533.6.013.4 533.696 3c6e7 3b3g2</p>
<p>AGARD Report 347 North Atlantic Treaty Organization, Advisory Group for Aeronautical Research and Development STATIC AND DYNAMIC STABILITY OF BLUNT BODIES H.C. DuBose 1961 27 pages, incl. 2 refs., 17 figs; plus discussion and bibliography of papers presented at the Stability and Control Meeting</p> <p>A description is given of the relationships between the flow fields and the static and dynamic stability of blunted-cone-cylinder-flare-type re-entry bodies at Mach numbers from 0.7 to 5.0. Effects of variations in some of the shape parameters on the dynamic stability are presented. It is shown that certain combinations of cone and flare angles result in instability in the transonic range. Also, comparison is made between free and forced oscillation data.</p> <p>P.T.O.</p>	<p>533.6.013.4 533.696 3c6e7 3b3g2</p>	<p>AGARD Report 347 North Atlantic Treaty Organization, Advisory Group for Aeronautical Research and Development STATIC AND DYNAMIC STABILITY OF BLUNT BODIES H.C. DuBose 1961 27 pages, incl. 2 refs., 17 figs; plus discussion and bibliography of papers presented at the Stability and Control Meeting</p> <p>A description is given of the relationships between the flow fields and the static and dynamic stability of blunted-cone-cylinder-flare-type re-entry bodies at Mach numbers from 0.7 to 5.0. Effects of variations in some of the shape parameters on the dynamic stability are presented. It is shown that certain combinations of cone and flare angles result in instability in the transonic range. Also, comparison is made between free and forced oscillation data.</p> <p>P.T.O.</p>	<p>533.6.013.4 533.696 3c6e7 3b3g2</p>

This Report is one in the Series 334-374, inclusive, presenting papers, with discussions, given at the AGARD Specialists' Meeting on 'Stability and Control', Training Center for Experimental Aerodynamics, Rhode-Saint-Genèse, Belgium, 10-14 April 1961, sponsored jointly by the AGARD Fluid Dynamics and Flight Mechanics Panels

This Report is one in the Series 334-374, inclusive, presenting papers, with discussions, given at the AGARD Specialists' Meeting on 'Stability and Control', Training Center for Experimental Aerodynamics, Rhode-Saint-Genèse, Belgium, 10-14 April 1961, sponsored jointly by the AGARD Fluid Dynamics and Flight Mechanics Panels

This Report is one in the Series 334-374, inclusive, presenting papers, with discussions, given at the AGARD Specialists' Meeting on 'Stability and Control', Training Center for Experimental Aerodynamics, Rhode-Saint-Genèse, Belgium, 10-14 April 1961, sponsored jointly by the AGARD Fluid Dynamics and Flight Mechanics Panels

This Report is one in the Series 334-374, inclusive, presenting papers, with discussions, given at the AGARD Specialists' Meeting on 'Stability and Control', Training Center for Experimental Aerodynamics, Rhode-Saint-Genèse, Belgium, 10-14 April 1961, sponsored jointly by the AGARD Fluid Dynamics and Flight Mechanics Panels